

Statistical mechanics of topological phase transitions in networks

Gergely Palla, Imre Derényi, Illés Farkas, and Tamás Vicsek
*Biological Physics Research Group of HAS and Department of Biological
Physics, Eötvös University, Pázmány P. stny. 1A, H-1117 Budapest, Hungary*
(October 22, 2018)

We provide a phenomenological theory for topological transitions in restructuring networks. In this statistical mechanical approach energy is assigned to the different network topologies and temperature is used as a quantity referring to the level of noise during the rewiring of the edges. The associated microscopic dynamics satisfies the detailed balance condition and is equivalent to a lattice gas model on the edge-dual graph of a fully connected network. In our studies – based on an exact enumeration method, Monte-Carlo simulations, and theoretical considerations – we find a rich variety of topological phase transitions when the temperature is varied. These transitions signal singular changes in the essential features of the global structure of the network. Depending on the energy function chosen, the observed transitions can be best monitored using the order parameters $\Phi_s = s_{\max}/M$, *i.e.*, the size of the largest connected component divided by the number of edges, or $\Phi_k = k_{\max}/M$, the largest degree in the network divided by the number of edges. If, for example the energy is chosen to be $E = -s_{\max}$, the observed transition is analogous to the percolation phase transition of random graphs. For this choice of the energy, the phase-diagram in the $[\langle k \rangle, T]$ plane is constructed. Single vertex energies of the form $E = \sum_i f(k_i)$, where k_i is the degree of vertex i , are also studied. Depending on the form of $f(k_i)$, first order and continuous phase transitions can be observed. In case of $f(k_i) = -(k_i + \alpha) \ln(k_i)$, the transition is continuous, and at the critical temperature scale-free graphs can be recovered. Finally, by abruptly decreasing the temperature, non-equilibrium processes (*e.g.*, nucleation, growth of particular topological phases) can also be interpreted by the present approach.

PACS numbers: 9.75.Hc, 05.70.Fh, 64.60.Cn, 87.23.Ge

I. INTRODUCTION

In recent years, the analysis of the network structure of interactions has become a popular and fruitful method used in the study of complex systems. Whenever many similar objects in mutual interactions are encountered, these objects can be represented as nodes and the interactions as links between the nodes, defining a network. The world-wide-web, the science citation index, and biochemical reaction pathways in living cells are all good examples of complex systems widely modeled with networks, and the set of further phenomena where the network approach can be used is even more diverse. In most cases, the overall structure of networks reflect the characteristic properties of the original systems, and enable one to sort seemingly very different systems into a few major classes of stochastic graphs [1, 2]. These developments have greatly advanced the potential to interpret the fundamental common features of such diverse systems as social groups, technological, biological and other networks. The effects of both the restructuring [3] and the growth [4] of the associated graphs have been considered, leading to a number of exciting discoveries about the laws concerning their diameter, clustering and degree distribution. Real networks typically exhibit both aspects (growth and rearrangement) one of which is usually dominating the dynamics. Here we concentrate on the evolution of graphs due to restructuring, but shall briefly discuss the growth regime as well.

Various interesting effects observed in networks can be interpreted using analogies with well understood phenomena studied in statistical physics. As a classical example, we mention the percolation phase transition in the Erdős-Rényi (ER)

random graph model [5, 6], which occurs by varying the average degree, $\langle k \rangle$, of the vertices around $\langle k \rangle = 1$. For $\langle k \rangle < 1$ the graph falls apart into small pieces, on the other hand for $\langle k \rangle \geq 1$ a giant connected component emerges (in addition to the finite components). Another subtle example is the mapping of a growing network model onto an equilibrium Bose gas [7]. For the latter model, under certain conditions a single node is allowed to collect a finite fraction of all edges, corresponding to a highly populated ground level and sparsely populated higher energies seen in Bose-Einstein condensation.

When connecting the graph theoretical aspects of networks to statistical physics, one can step further from the analogies by directly defining *statistical ensembles for graphs*. The use of a statistical mechanical formalism for the changes in graphs being in an equilibrium-like state is expected to provide a significantly deeper insight into the processes taking place in systems being in a saturated state and, as such, dominated by the fluctuating rearrangements of links between their units.

As an example, let us take a given number of units interacting in a “noisy” environment. These units can be people, firms, genes, *etc.* The probability for establishing a new or ceasing an existing interaction between two units depends on both the noise and the advantage gained (or lost) when adopting the new configuration. In this picture, a global transition in the connectivity properties can occur as a function of the level of noise. For instance, if the conditions are such that the interactions between the partners become more “conservative” (safer choices are more highly valued), then – as we show later – a transition from a less ordered to a more ordered network configuration can take place. In particular, it has been argued [8] that depending on the level of certain types of un-

certainties (expected fluctuations) business networks reorganize from a star-like topology to a system of more cohesive, highly clustered ties.

There are several possible ways to define the statistical ensemble of networks. In [9, 10], the members of the ensemble were identified by the Feynman diagrams of a field theory in zero dimensions (called “minifield”), and the weights of the graphs were given by the corresponding amplitudes calculated using the standard Feynman rules. The ensemble obtained this way was characterized by the fractal and spectral dimensions, and the dependence of the topology of the graphs on these two parameters was discussed. The authors argued that in the parameter plane of two parameters related to the fractal and spectral dimension, the region of generic graphs and the region of crumpled graphs are separated by a line; and on this separating line scale-free networks appear. An alternative definition for the partition function was proposed by Berg and Lässig in [11], resulting in a simpler formalism, analogous to the statistical mechanics of classical Hamiltonian systems. They introduced a Hamiltonian for networks, and also a parameter β playing the role of inverse temperature. The weights of different graphs in the partition function were obtained from these two quantities as in classical statistical mechanics. These studies showed that Hamiltonians beyond the single vertex form (where terms depending on connectivities between the vertices also appear) lead to correlations between the vertices for large β . A similar model leading to interesting results was presented in [12], where the Hamiltonian depended on the ratios of the degrees of neighboring vertices, and the dynamics favored disassortative mixing and high clustering. The system organized itself into three phases depending on one parameter: the exponential, scale-free and hub-leaves states were produced, respectively. However, the non-uniform selection of links at the rewiring in this model makes it impossible to satisfy the detailed balance condition.

In this paper we analyze the reorganization of networks from the point of view of *topological phase transitions*, i.e., transitions in the graph structure as a function of *temperature*, the quantity representing the level of noise during the restructuring process of the network. For clarity we note that our studies concern a class of phenomena that are clearly different from the phase transitions investigated by applying models of statistical mechanics originally defined on regular lattices to an underlying (static) random network structure [13, 14, 15], or the phase transitions observed in growing networks [7, 16], or quasi-static networks [17]. Topological phase transitions are accompanied by singularities in the thermodynamic functions derived from the partition function of the statistical graph ensemble and can be characterized by a drastic change in an appropriate order parameter. Our statistical ensemble (similarly to the one presented in Ref. [11]), is defined by introducing an *energy* that accounts for the advantage or loss during the rearrangement. In our description, this energy may depend on either global properties of the network, or single vertex degrees as well.

The use of Hamiltonian formalism also provides a general

frame for the optimization of network structure (for examples of network optimization problems see [18, 19]). To find the optimal configuration for a given task, the system has to be cooled, using an appropriate energy function.

This article is a direct extension of our previous work [20]; covering more details, results, and new approaches. The paper is organized as follows: in Sec. II we define the canonical ensemble of the networks together with the partition function and other essential thermodynamic quantities. In Sec. III we discuss the numerical methods used to study the phase transitions. In Sec. IV we present the phase transitions obtained for energies that depend on global properties, and Sec. V is devoted to two interesting cases of single vertex energies. In Sec. VI we discuss briefly the grand canonical ensemble of networks and we conclude in Sec. VII.

II. STATISTICAL MECHANICS OF NETWORKS

We shall consider a set, $\{g_a\}$, of *undirected graphs*, containing N nodes and M links. Each graph g_a can be represented by the *adjacency matrix* A_{ij}^a , where $A_{ij}^a = 1$ if vertices i and j are connected and it is zero otherwise. In a heat bath at temperature T , the *canonical ensemble* of these graphs (in analogy with that proposed in [11]), can be defined by the partition function

$$Z(T) = \sum_{\{g_a\}} e^{-E_a/T}, \quad (1)$$

where E_a is the *energy* assigned to the different configurations.

The restructuring processes of the network can be interpreted via the following physical picture: The basic event of rearrangement is the reallocation of a randomly selected edge (link) to a new position either by “diffusion” (keeping one end of the edge fixed and connecting the other one with a new node) or by removing the given edge and connecting two randomly selected nodes. Then, the energy difference $\Delta E_{ab} = E_b - E_a$ between the original g_a and the new g_b configurations is calculated and the reallocation is carried out following the Metropolis algorithm [21]. If the energy of the new graph is lower than that of the original one, the reallocation is accepted; if the new energy is higher, the reallocation is accepted only with probability $e^{-\Delta E_{ab}/T}$. This way, in the $T \rightarrow \infty$ limit the dynamics converges to a totally random rewiring process, and thus, the classical ER random graphs are recovered. On the other hand, at low temperatures the topologies with lowest energy occur with enhanced probability. The resulting dynamics, by construction, satisfies the detailed balance condition [21].

This network rearrangement is formally equivalent to a *Kawasaki type lattice gas* dynamics with conserved number of particles moving on a special lattice, which is the edge-dual graph of the fully connected network [6, 22]. The sites of this lattice are the possible $N(N - 1)/2$ connections between the

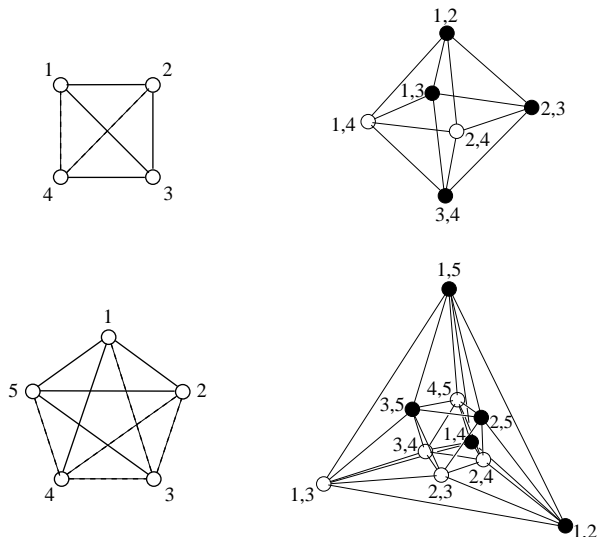


FIG. 1: Two simple examples of graphs (left hand side) and the corresponding edge-dual graphs (right hand side). The full spheres in the edge-dual graphs represent occupied sites, corresponding to existing bonds in the original graph (drawn with solid lines), and the hollow spheres are the empty sites, corresponding to absent bonds (represented by dashed lines) in the original network. The rewiring of an edge in the original graphs is equivalent to the displacement of the corresponding particle on the edge-dual graph.

vertices, and the particles wandering on the sites are the M edges, as shown in Fig. 1.

The partition function (1) contains many terms corresponding to *topologically equivalent* graphs: these graphs can be simply transformed into one another by an adequate permutation of the indexing. Since we consider energies E_α that depend only on the topology t_α , it is natural to rewrite the partition function in a form where the summation runs through all possible topologies:

$$Z(T) = \sum_{\{t_\alpha\}} \mathcal{N}_\alpha e^{-E_\alpha/T}. \quad (2)$$

Here we introduced \mathcal{N}_α to count the number of configurations belonging to topology t_α . Expression (2) can be rewritten as

$$Z(T) = \sum_{\{t_\alpha\}} e^{-E_\alpha/T + \ln(\mathcal{N}_\alpha)} = \sum_{\{t_\alpha\}} e^{-F_\alpha/T}, \quad (3)$$

$$F_\alpha = E_\alpha - TS_\alpha, \quad (4)$$

$$S_\alpha = \ln(\mathcal{N}_\alpha), \quad (5)$$

where F_α is the free energy and S_α is the entropy of the topology t_α .

We are interested in the possible singularities in the thermodynamic functions derived from the partition function above, since they, if there are any, correspond to phase transitions in the topology of the associated networks. These transitions can be best monitored by introducing a suitable *order parameter*. As we are primarily interested in the transitions between dispersed and compact states, a natural choice can be either

$\Phi = \Phi_s = s_{\max}/M$, the number of edges of the largest connected component of the graph s_{\max} normalized by the total number of edges M , or $\Phi = \Phi_k = k_{\max}/M$, the highest degree in the graph k_{\max} divided by M . We also introduce the corresponding conditional free energy $F(\Phi, T)$ via

$$e^{-F(\Phi, T)/T} = Z(\Phi, T) = \sum_{\{g_\alpha\}_\Phi} e^{-E_\alpha/T}, \quad (6)$$

where $\{g_\alpha\}_\Phi$ is a subset of $\{g_\alpha\}$, consisting of all the graphs with order parameter Φ . A phase transition, where a rapid change occurs in the order parameter from $\Phi = 0$ towards higher values, is also accompanied by a shift of the minimum of the conditional free energy $F(\Phi, T)$. A sudden change in the position of the global minimum signals a discontinuous (first order) phase transition, whereas a gradual shift indicates either a crossover or a continuous phase transition.

In the next section we briefly discuss the numerical methods used to study topological phase transitions.

III. NUMERICAL METHODS

III. A) Exact enumeration method

The numerical results shown in this paper were obtained by two alternative methods. Motivated by the success of a similar approach used in random-walks, percolation, and polymers related problems [23, 24, 25, 26], for small systems we evaluated the partition function together with the probability of every individual state via an *exact enumeration method*. In this approach, first all possible connected configurations with a given number of edges are generated successively up to M : the graphs with $m + 1$ edges are constructed from the graphs with m edges either by linking a new vertex to one of the old vertices, or by linking two previously unconnected vertices. Next, all possible configurations containing M edges are obtained from the combination of smaller connected graphs, with sizes up to M . Finally, \mathcal{N}_α is calculated for each topology t_α by counting the number of possible permutations chosen to label the vertices in the state. (For more details and a simple example, see appendix A). The probability p_α , of a topology t_α then can be obtained from

$$p_\alpha = \frac{\mathcal{N}_\alpha e^{-E_\alpha/T}}{Z}. \quad (7)$$

Once the set of possible states with appropriate probabilities has been constructed, one can evaluate the expectation value of any \mathcal{Q} thermodynamic quantity using

$$\langle \mathcal{Q} \rangle = \sum_{t_\alpha} \mathcal{Q}(t_\alpha) p_\alpha. \quad (8)$$

The advantage of this technique, beside producing exact results, is that the set of \mathcal{N}_α has to be calculated only once, independently of the energy functions considered, in contrast to Monte-Carlo simulations, where the simulation has to be

restarted from the beginning every time we introduce a new type of energy. This method is limited by the rapid growth of the number of topologies with M . For networks of size seen in the real world ($M > 10^2$) the realization of this method is clearly unfeasible.

III. B) Monte-Carlo simulations

The lattice gas model defined on the edge-dual graph of the fully connected network relaxes slowly, because interactions are dense [31] and the energy minima are sometimes localized in hardly accessible parts of the phase space of the system. A good example is the transition from a classical random graph – stable at high temperatures – to a star, which is stable at low temperatures. The simplest Monte-Carlo rewiring simulation (discussed in Sec. II.) tries to move a randomly chosen edge to a randomly chosen new location. However, this method is very inefficient, if one would like to simulate the condensation of edges into a star in a large system.

There are several simulation tools that can help to achieve faster convergence. We have used the so-called parallel tempering (also called exchange Monte-Carlo) method in several cases [27]. Except for first-order transitions, this algorithm can be used well to measure the transition at an acceptable speed and high precision.

The algorithm can be viewed as an improved version of simulated annealing. Several replicas of the system are simulated simultaneously, and each of them is connected to a separate heat bath. A replica in a hot heat bath will explore the "large-scale" structure of phase space, and the motion of a replica in a cold heat bath will be restricted to a small part of phase space, where it will explore the deep but narrow energy wells.

In the exchange Monte-Carlo method, after a given number of conventional update steps within each replica, exchange steps are made. Two replicas (with neighboring temperatures) are chosen at random, and a Monte-Carlo-type decision is made whether the two replicas should be exchanged, *i.e.*, their temperatures should be swapped. With Metropolis dynamics, if the product of the energy difference between the two replicas (ΔE) and the difference of inverse temperatures ($\Delta\beta$) is positive, then this exchange is accepted, otherwise it is accepted only with probability $e^{\Delta\beta \Delta E}$. That is, a replica with a high energy and a low inverse temperature (*i.e.*, high temperature) will be more likely to remain in its own heat bath, whereas a replica with a high energy and a high inverse temperature (*i.e.*, low temperature) will be likely to be "put" into a heat bath with a higher temperature.

We shall now move on to review some of energy functions, that lead to phase transitions, when the temperature is changed from zero to infinity at constant $\langle k \rangle$. Since at $T = \infty$ the entropically favorable graphs dominate, a minimum requirement for the energy function is that the configurations with the lowest energy must also have low entropy. We divide the investigated energy functions into two categories. In the first category we put the energies that depend on component sizes

in the graph, the other group contains the single-vertex energies.

IV. CLUSTER ENERGIES

As mentioned in the introduction, the classical random graph model (corresponding to $T \rightarrow \infty$) exhibits a phase transition when the average degree of the vertices, $\langle k \rangle = 2M/N$, is varied around $\langle k \rangle = 1$. For $\langle k \rangle < 1$, the network consists of small, disconnected clusters, on the other hand, for $\langle k \rangle \geq 1$ a giant connected component emerges in the graph collecting a finite portion of the edges. Near the critical point the size of the giant component scales as $(\langle k \rangle - 1)M$.

Based on the lattice gas analogy we expect that if $\langle k \rangle < 1$, then for a suitable choice of the energy (one that rewards clustering) a similar dispersed-compact phase transition occurs at a finite temperature $T(\langle k \rangle)$. Such a transition can be best monitored by the order parameter $\Phi_s = s_{\max}/M$ (the number of edges in the largest connected component s_{\max} divided by the total number of edges), often used in graph theory [28].

The most obvious energy satisfying the above requirement is a monotonically decreasing function $E = f(s_{\max})$. In this case the energy is independent of the distribution of the size of smaller clusters, or of the structural details of the largest cluster: only the size of the largest cluster matters. The entropic part of the conditional free energy in this case can be estimated by counting the number of configurations at given s_{\max} . The number of different connected configurations of size s_{\max} can be estimated as $s_{\max}^{s_{\max}}$ to leading order [29], (for an intuitive derivation see appendix B). This term has to be multiplied by the number of possible selections of these s_{\max} vertices out of N , which is simply N over s_{\max} . The $M - s_{\max}$ left-out edges can be placed anywhere between the $N - s_{\max}$ remaining vertices, with the restriction that they cannot form clusters larger than s_{\max} . Since we consider $s_{\max} = \Phi_s M$ to be an extensive quantity and the typical size of the largest component of these left-out edges scales slower than M , this constraint can be neglected. Hence, the contribution from the left-out edges can be well estimated by an $(N - s_{\max})^2/2$ over $(M - s_{\max})$ factor. If we combine these factors together, then in the thermodynamic limit (when $N, M \rightarrow \infty$, $\langle k \rangle = \text{const.}$) we can write

$$\mathcal{N}_{\text{clus}} \approx (\Phi_s M)^{\Phi_s M} \binom{N}{\Phi_s M} \left(\frac{(N - \Phi_s M)^2}{2} \right)^{M - \Phi_s M}. \quad (9)$$

Since the energy of the system is a function of the order parameter Φ_s itself, the conditional free energy $F(\Phi_s, T)$ can be expressed as

$$e^{-F(\Phi_s, T)/T} = \mathcal{N}_{\text{clus}} e^{-f(\Phi_s)/T} = e^{-[f(\Phi_s) - T \ln \mathcal{N}_{\text{clus}}]/T} \quad (10)$$

By using Stirling's formula [$l! \approx (l/e)^l \sqrt{2\pi l}$] to approximate the factorials and neglecting terms of $\mathcal{O}(\ln N)$, for $\ln \mathcal{N}_{\text{clus}}$ we get

$$\ln \mathcal{N}_{\text{clus}} \approx \text{const.} + \left[1 + \ln \frac{2M}{N} - \frac{2M}{N} \right] \Phi_s M$$

$$+ \left[\frac{3M}{2N} - \frac{1}{2} - \frac{M^2}{N^2} \right] \Phi_s^2 M. \quad (11)$$

By replacing $2M/N$ with $\langle k \rangle$ in the expression above, the resulting conditional free energy can be expressed as

$$F(\Phi_s, T) \approx f(\Phi_s M) + MT \left\{ [\langle k \rangle - 1 - \ln(\langle k \rangle)] \Phi_s + \left[\langle k \rangle^2 - 3 \langle k \rangle + 2 \right] \frac{\Phi_s^2}{4} \right\}. \quad (12)$$

The simplest choice for an energy function that depends only on the size of the largest component is

$$f(s_{\max}) = -s_{\max} = -\Phi_s M. \quad (13)$$

In this case it can be clearly seen from Eq. (12) that as long as

$$T > T_c(\langle k \rangle) = \frac{1}{\langle k \rangle - 1 - \ln(\langle k \rangle)}, \quad (14)$$

the free energy has a minimum at $\Phi_s = \Phi_s^*(T) = 0$, *i.e.*, the configuration is dispersed (see main panel of Fig. 2). When the temperature drops below $T_c(\langle k \rangle)$, the minimum moves away from $\Phi_s = 0$ and a giant component appears. Near the critical temperature $T_c(\langle k \rangle)$, the order parameter at the minimum of the free energy can be estimated from Eq. (12) as

$$\Phi_s^*(T) = 2 \frac{T^{-1} - T_c^{-1}(\langle k \rangle)}{\langle k \rangle^2 - 3 \langle k \rangle + 2}, \quad (15)$$

indicating that we are dealing with a *continuous topological phase transition* (see inset of Fig. 2).

Topological phase transitions of first order are also expected to occur for other forms of cluster energies. For example, when $f(s_{\max})$ starts with a zero (or positive) slope. In such a case, the behavior of the conditional free energy at very high and very low temperatures is similar to the previous case: when $T \rightarrow \infty$, the energy term $f(s_{\max})$ can be neglected in (12), and the entropic term has a minimum at $\Phi_s = 0$, which is the dispersed state. In contrast, when $T \rightarrow 0$, only the energy term remains, resulting a minimum in $F(\Phi_s, T)$ at $\Phi_s = 1$, the compact state. However, there is also an intermediate temperature range, where $F(\Phi_s, T)$ given by (12) starts as an increasing function at $\Phi_s = 0$ (since the linear term in the entropy dominates for small Φ_s), then reaches its maximum somewhere in the $[0, 1]$ interval and continues as a decaying function from that point on (since the higher order decaying terms in the energy overcome the increasing terms at larger Φ_s). As a consequence, the conditional free energy has two competing minima in the $[0, 1]$ interval, a meta-stable and a globally stable. The coexistence of stable and meta-stable minima at the transition between the phases is a characteristic of first order phase transitions. A simple function of this type is $f(s_{\max}) = -s_{\max}^2$. For this choice of the energy, our numerical results are shown in Fig.3. The hysteresis

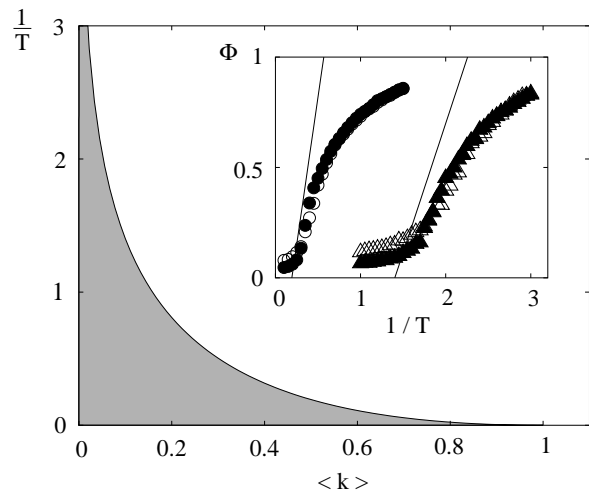


FIG. 2: The phase diagram and the order parameter for the $E = -s_{\max}$ energy. Main panel: The white and shaded areas correspond to the ordered phase (containing a giant component) and the disordered phase, respectively, as given by Eq. (14). Inset: The order parameter $\Phi = \Phi_s = s_{\max}/M$ obtained from Monte-Carlo simulations as a function of the inverse temperature for $\langle k \rangle = 0.1$ (triangles) and $\langle k \rangle = 0.5$ (circles). Each data point is an ensemble average of 10 runs, time averaged between $t = 100N$ and $500N$ Monte-Carlo steps. The open and closed symbols represent $N = 500$ and $1,000$ vertices, respectively. The critical exponent, in agreement with the analytical approximations (solid lines), was found to be 1.

appearing between cooling and heating supports the theoretical considerations about the coexisting minima that indicate a first order phase transition, summarized in the inset of Fig.3. The analytical conditional free energy gained by substituting $f(s_{\max}) = -s_{\max}^2$ into (12) has a single minimum, when $T < 80$ and when $T > 430$, in former case at the dispersed state ($\Phi_s = 0$), in latter case at the connected state ($\Phi_s = 1$). At intermediate temperatures these two minima coexist, predicting a first order phase transition somewhere in the middle part of this temperature interval. The transition regime $170 < T < 270$ observed in the MC simulation is compatible with the analytical result, since one does not expect the simulation to reveal the meta-stable state beside its dominant stable counterpart in case of a very significant difference between the depths of the according minima in the free energy.

We have also investigated the case of $f(s_{\max}) = -s_{\max} \ln(s_{\max})$, both analytically and numerically. Similarly to the previous case, it can be shown that there is a temperature regime, where the conditional free energy as a function of Φ_s has two competing minima, hence the transition is of first order.

Since the energy $E = f(s_{\max})$ depends on a global quantity (the size of the largest connected component) it might be also reasonable to define the energy of the graph as $E = \sum_j f(s_j)$, where the summation goes over each component and s_j denotes the number of edges in the j th one. The total number of edges, $M = \sum_j s_j$, is conserved by the dynamics, hence $f(s_j)$ must decrease faster than linear to promote compactification. When a single giant component (containing the

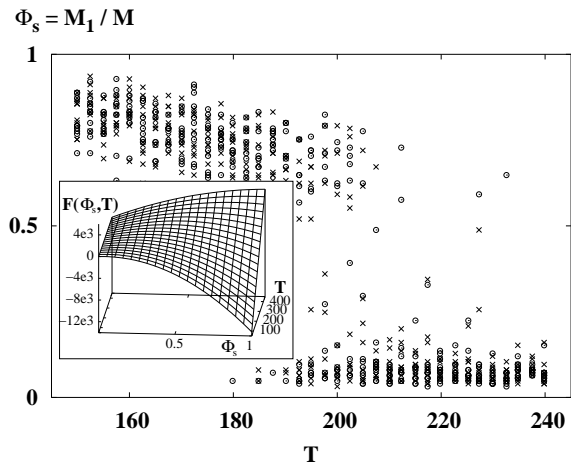


FIG. 3: If the energy of the graph is $E = -s_{\max}^2$, then the order parameter, $\Phi_s = M_1/M$, shows a first order transition. (M_1 is the number of edges in the largest component of the graph.) Each point gives the value of Φ_s averaged between $t = 490N$ and $t = 500N$ Monte-Carlo steps in a graph started at $t = 0$ from an Erdős-Rényi random graph (o) or a star (\times). The simulated graph had $N = 500$ vertices and $M = 125$ edges. The inset shows the behavior of the analytical free energy obtained from (12) using the same parameters. The temperature interval in which the two minima (at $\Phi_s = 0$, corresponding to the connected state and at $\Phi_s = 1$, corresponding to the dispersed state) coexist is fully compatible with the numerical findings for the transition regime.

majority of the edges) emerges, its energy $f(s_{\max})$ dominates the energy of the entire graph, and, as a good approximation, the above analysis for $E = f(s_{\max})$ can be repeated, leading to first order and continuous phase transitions. For the case of $E = -\sum_{i=1}^{N_c} s_i^2$, our numerical results are presented in Fig.4, showing a first order phase transition.

For the $E = -\sum_{i=1}^N s_i \ln(s_i)$ energy – similarly to the case of the $E = -s_{\max} \ln(s_{\max})$ energy – we found a first-order transition between the ordered phase (present at low temperatures) and the disordered phase (high temperatures). Results are shown in Fig. 5.

V. SINGLE VERTEX ENERGY FUNCTIONS

Next we turn to another important class of the energy functions, where the energies are assigned to the vertices rather than to the connected components of the graph:

$$E = \sum_{i=1}^N f(k_i), \quad (16)$$

where k_i denotes the degree (number of neighbors) of vertex i . This energy is consistent with a dynamics in which the change of the degree of a vertex depends only on the structure of the graph in its vicinity. The fitness of an individual vertex depends on its connectivity. The most suitable order parameter for this class of graph energy is $\Phi = \Phi_k = k_{\max}/M$. Again,

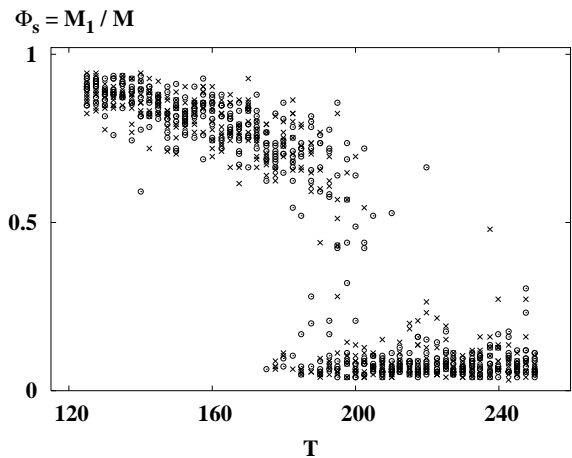


FIG. 4: The order parameter, $\Phi_s = M_1/M$, for the $E = -\sum_{i=1}^{N_c} s_i^2$ energy. (M_1 is the number of edges in the largest component and N_c is the number of components in a graph.) Each point shows the value of Φ_s after $t = 200N$ Monte-Carlo steps in a graph started at $t = 0$ from an Erdős-Rényi random graph (o) or a star (\times). The simulated graph had $N = 500$ vertices and $M = 125$ edges. Observe that for intermediate temperatures there are two distant groups of states with high stability (at $\Phi_s \approx 0.6 - 0.9$ and $\Phi_s \approx 0 - 0.15$), and Φ_s values in the region between these two rarely occur, *i.e.*, a first order transition was found.

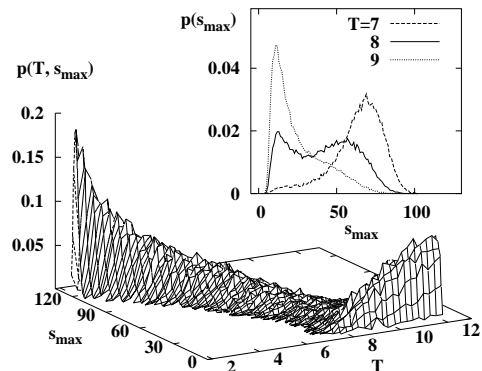


FIG. 5: Distribution of the size of the largest graph component, s_{\max} , if the $E = -\sum_{i=1}^N s_i \ln(s_i)$ energy is used. Main panel. At low temperatures the distribution of the largest component has one maximum at large values of s_{\max} , this is the ordered phase. At high temperatures, the largest component is small: the graph is disordered. Inset. Using a higher resolution, one can observe that the transition from the low-temperature peak ($T = 7$) to the high-temperature peak ($T = 9$) happens via a bimodal distribution ($T = 8$, indicated by a solid line). This indicates that the conditional free energy of the system has two competing minima at the intermediate temperature, and the transition is of first order. The graphs used for the simulations had $N = 500$ vertices and $M = 125$ edges. Averages were taken for 10 (main panel) or 200 (inset) simulation runs between simulation times of $t = 200N$ and $t = 400N$ Monte-Carlo steps using time steps of $t = N$.

due to the conservation of the number of edges, $M = \sum_i k_i$, the single vertex energy $f(k_i)$ should decrease faster than $-k_i$, if aggregation is to be favored.

We introduce an alternative form for single vertex energies:

$$E = \sum_{i=1}^N \sum_{i'} g(k_{i'}), \quad (17)$$

where i' runs over all vertices that are neighbors of vertex i . In this interpretation, the fitness of an individual vertex depends on the connectivities of its neighbors, and vertex i collects an energy $g(k_{i'})$ from each of its neighbors. These neighbors in turn will all collect $g(k_i)$ from vertex i , therefore the total contribution to the energy from vertex i is $k_i g(k_i)$. Thus, by using

$$f(k_i) = k_i g(k_i), \quad (18)$$

the two alternative forms of the single vertex energy, (16) and (17), become equivalent.

V. A) The energy $E = -\sum k_i^2$: mapping to the Ising-model

A natural choice for the energy of single vertex type is the following. Assign the negative energy $-J$ to all pairs of edges that share a common vertex at one end. The total energy of a given configuration is then

$$E = -\frac{J}{2} \sum_{i=1}^N k_i(k_i - 1) = -\frac{J}{2} \sum_{i=1}^N k_i^2 + \frac{1}{2}JM, \quad (19)$$

corresponding to $f(k_i) = -(J/2)k_i^2$, (or equivalently, to $g(k_i) = -(J/2)k_i$). The constant term in (19) does not play any role in the dynamics, hence it can be omitted. This form of the energy is in full analogy with the usual definition of the energy

$$E = -J \sum_{\langle \alpha, \beta \rangle} n_\alpha n_\beta \quad (20)$$

of a lattice gas on the edge-dual graph of the fully connected network with nearest neighbor attraction. The summation here runs over all adjacent pairs of lattice sites (corresponding to possible edges between the vertices of the original graph), and $n_\alpha = 1$ if site α is occupied and 0 otherwise. When this energy is applied to lattices, we recover the standard lattice gas model of nucleation of vapors. The negative energy unit $-J$ associated with a pair of edges sharing a vertex in the original graph is equivalent to the binding energy between the corresponding occupied nearest neighbor sites on the edge-dual graph. By measuring the energies (and temperature) in units of J we can set $J = 1$, without loosing generality. Thus, from now on J will be omitted.

The lattice gas representation can be further transformed to an Ising-model-representation by introducing the $s_\alpha \in [-1, 1]$

spin-like variables connected to n_α as $n_\alpha = (1 + s_\alpha)/2$. The energy with the help of the spins is expressed as

$$E = -\frac{1}{4} \sum_{\langle \alpha, \beta \rangle} s_\alpha s_\beta - \frac{1}{2} \sum_{\alpha=1}^{N(N-1)/2} s_\alpha - \frac{1}{8} N(N-1)(N-2), \quad (21)$$

since the total number of lattice sites equals $N(N-1)/2$, and the number of adjacent pairs of lattice sites is $N(N-1)(N-2)/2$. This is similar to a ferromagnetic Ising-model in an external magnetic field. If the number of occupied sites in the lattice gas picture equals the number of unoccupied sites, the contribution from the external magnetic field vanishes in the Ising-model picture. However, in the thermodynamic limit, where $N \rightarrow \infty$, $M \rightarrow \infty$, $\langle k \rangle = 2M/N = \text{const.}$, this condition cannot be fulfilled, since the total number of sites scales as N^2 , whereas the number of particles scales as M with the system size.

For the particular form of $f(k_i)$ chosen, the topology with the lowest overall energy is a ‘‘star’’ (for simplicity, we consider $M < N$), where all the M edges are connected to single node. The form of the conditional free energy in this case can be estimated as follows. In the $\Phi_k > 1/2$ regime, where the system contains a star of size larger than $M/2$, the energy of this star dominates the rest of the graph. Therefore, in the thermodynamic limit, we neglect this latter contribution to the total energy and approximate the energy of the graph by that of the largest star. Now we estimate the number of possible configurations for a given value of Φ_k . In case of a star with $K = \Phi_k M$ arms, the central vertex can be chosen from N different vertices. Once this is fixed, K edges have to be distributed among the $N-1$ possible links between the other vertices and the central one, yielding a factor of $N-1$ over K . The rest of the edges that are not part of the star can be placed anywhere between the $N-1$ (non-central) vertices, contributing a factor of $(N-1)(N-2)/2$ over $(M-K)$.

$$\mathcal{N}_{\text{star}}(K) \approx N \binom{N-1}{K} \binom{(N-1)(N-2)/2}{M-K} \approx N \binom{N}{K} \binom{N^2/2}{M-K}. \quad (22)$$

Again, we use Stirling’s formula to approximate the factorials, and neglect terms of the order $\mathcal{O}(\ln N)$ yielding

$$\begin{aligned} \ln \mathcal{N}_{\text{star}} \approx M & \left[\frac{N}{M} \ln \frac{N}{M} + \frac{N^2}{2M} \ln \frac{N^2}{2M} \right. \\ & - \left(\frac{N}{M} - \Phi_k \right) \ln \left(\frac{N}{M} - \Phi_k \right) \\ & - \Phi_k \ln \Phi_k - (1 - \Phi_k) \ln(1 - \Phi_k) \\ & \left. - \left(\frac{N^2}{2M} - 1 + \Phi_k \right) \ln \left(\frac{N^2}{2M} - 1 + \Phi_k \right) \right] \quad (23) \end{aligned}$$

In the thermodynamic limit, to leading order we receive

$$\ln \mathcal{N}_{\text{star}}(x) \approx -\Phi_k M \ln(N), \quad (24)$$

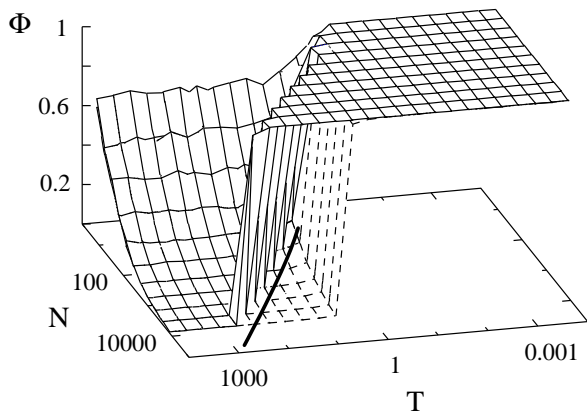


FIG. 6: The order parameter $\Phi = \Phi_k = k_{\max}/M$ as a function of the temperature and the system size for $E = \sum_i -k_i^2/2$ and $\langle k \rangle = 0.5$. The simulations were started either from a star (corresponding to $T = 0$, solid line) or a classical random graph ($T = \infty$, dashed line). Each data point represents a single run, time averaged between $t = 100N$ and $200N$ Monte-Carlo steps. The thick solid line shows the analytically calculated spinodal $T_1 = M/\ln(N)$.

where the Φ_k independent terms were dropped. The resulting conditional free energy is expressed as:

$$F(\Phi_k, T) \approx f(\Phi_k M) + \Phi_k M T \ln(N). \quad (25)$$

In the present case, with the $f(k_i) = -k_i^2$ energy, (25) can be written as

$$F(\Phi_k, T) \approx M [-\Phi_k^2 M + \Phi_k T \ln(N)]. \quad (26)$$

Note that this approximation would be valid even for $\Phi_k < 1/2$, if the energy of the graph was simply defined as $E = f(k_{\max})$.

The parabola given by Eq. (26) has a maximum at $\Phi_k = T/M \ln(N)$. When $T \rightarrow 0$, this maximum also shifts towards zero and $F(\Phi_k, T)$ becomes a descending parabola on the $[0, 1]$ interval. This means that the minimum of the free energy is at $\Phi_k = 1$, the star configuration. In contrast, when the temperature goes above the $T_1 = M/\ln(N)$ spinodal point (thick solid line in Fig. 6), the maximum moves out of the $[0, 1]$ interval and the free energy becomes an ascending parabola, resulting in a minimum at a low value of Φ_k (corresponding to an ER random graph). However, this value cannot be deduced from Eq. (26), because it is a valid approximation only for $\Phi_k > 1/2$. For intermediate temperatures the maximum of the parabola separates the two extreme topologies: the dispersed random graph and the star. One of these two extreme states is meta-stable and the other one is stable. Due to the limited validity of Eq. (26), the stability of these configurations can be studied only for temperatures where the maximum of the parabola is well inside the $[1/2, 1]$ interval.

The scenario of the transition from a dispersed state to the star configuration (see above) indicates that it is a *first order phase transition*. This is well supported by the results of both the exact enumeration method and Monte-Carlo simulations. For small systems, the conditional free energy

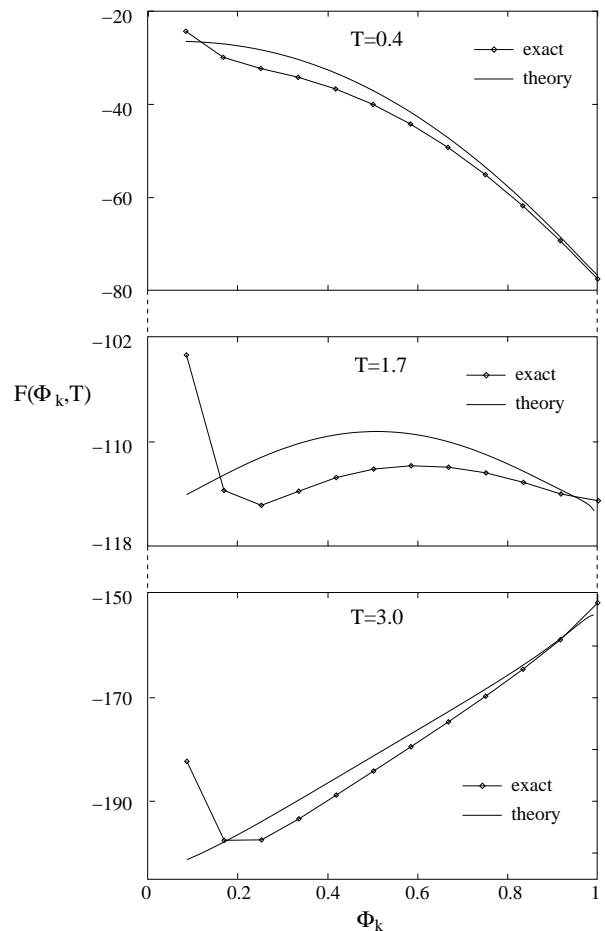


FIG. 7: The picture of the conditional free energy at three different temperatures for the $f(k_i) = -k_i^2$ energy, obtained from the exact enumeration method plotted together with the prediction of our simple theoretical analysis for $M = 12$, $N = 48$. At low temperatures $F(\Phi_k, T)$ is a descending function on the $[0, 1]$ with a minimum at $\Phi_k = 1$, the star configuration (top figure), on the other hand for high temperatures, it becomes ascending for most part, with a minimum at low Φ_k , the dispersed states (bottom picture). There is an intermediate temperature regime in between, where the maximum of $F(\Phi_k, T)$ separates two competing minima (middle figure), hence this phase transition is of first order.

was evaluated via the exact enumeration method for various temperatures, and was found to be in qualitative agreement with the prediction of the theoretical analysis, as demonstrated in Fig. 7. The three different temperature regimes described in the previous paragraph can be recognized in the behavior of the exact $F(\Phi_k, T)$ as well. Furthermore, in the intermediate temperature regime, where the conditional free energy has two competing minima, the spinodal curve can also be constructed as is shown in Fig. 8. For large enough systems, in MC simulations a sudden change of the order parameter between zero and one can be observed as shown in Fig. 6. The hysteresis appearing between cooling and heating is consistent with a first order transition.

V. B) The energy $E = -\sum k_i \ln k_i$: continuous phase-

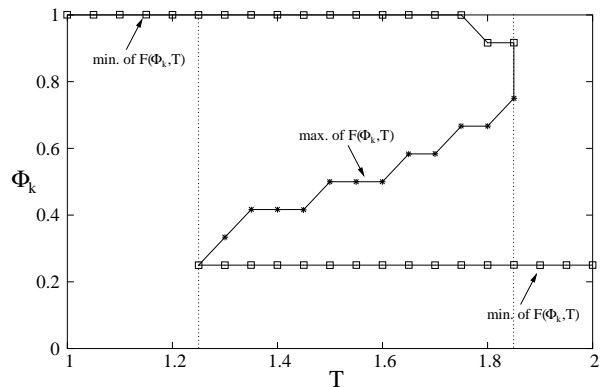


FIG. 8: The spinodal curve obtained from the exact enumeration method with $E = -\sum_i k_i^2$, for $M = 12, N = 48$. At low and high temperatures, the conditional free energy $F(\Phi_k, T)$ has a single minimum (plotted with squares). At intermediate temperatures (in between the two dotted lines) there are two competing minima. In this latter temperature regime, the spinodal curve is obtained by plotting the maximum of $F(\Phi_k, T)$ (represented by stars), besides the two minima.

transition

Another application-motivated choice for the single vertex energy is $f(k_i) = -k_i \ln(k_i)$, or equivalently, $g(k_i) = -\ln(k_i)$, inspired, in part, by the logarithmic law of sensation. It is the logarithm of the degree of a vertex that its neighbors can sense and benefit from. In this case the configuration with the lowest energy is a fully connected subgraph [or almost fully connected if M cannot be expressed as $n(n-1)/2$]. On the other hand, the star configuration is also quite favorable, since the energy of both the maximal possible star and of the maximal possible fully connected subgraph scales as $-M \ln M$ to leading order. Amongst the subdominant terms in the energy, there is a difference in the order of $\sqrt{M} \ln \sqrt{M}$ between the two, in favor of the fully connected subgraph. As before, we choose the order parameter to be $\Phi = \Phi_k = k_{\max}/M$, since this can easily distinguish between these two configurations: $k_{\max} \approx \sqrt{2M}$ for a fully connected subgraph counting M edges, and $k_{\max} \approx M$ for a star.

Our MC simulations demonstrate (Fig. 9) that as we cool down the system, first the edges of the dispersed random graph assemble to form a configuration with a few large stars (sharing most of their neighbors), and then at lower temperatures the graph is rearranged into an almost fully connected subgraph. This is consistent with the fact that beside the slight energetical disadvantage, the star configuration is entropically more favorable when compared to the fully connected subgraph; therefore the latter configuration can take over only at very low temperatures. The hysteresis near the few large star vs. fully connected subgraph transition suggests that it is a *first order phase transition*. On the other hand, the transition between the dispersed state and the few large stars is accompanied by a singularity in the heat capacity (also seen with the exact enumeration method), and no hysteresis is observed,

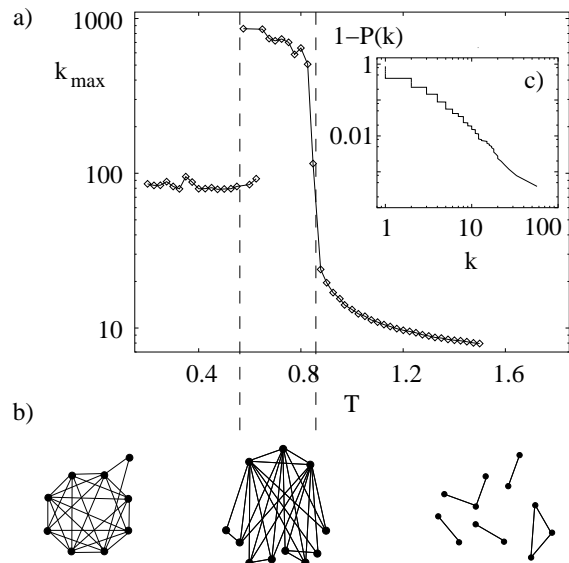


FIG. 9: Phases of the graph when the energy is $E = -\sum_i k_i \ln(k_i)$. (a) The largest degree k_{\max} for $N = 10, 224$ vertices and $M = 2, 556$ edges. Each data point represents a single run, time averaged between $t = 5, 000N$ and $20, 000N$ MC steps. The data points are connected to guide the eye. There is a sharp, continuous transition near $T = 0.85$ and a first-order transition (with a hysteresis) around $T = 0.5 - 0.6$. (b) The three different plateaus in (a) correspond to distinct topological phases: $k_{\max} = \mathcal{O}(1)$ to the classical random graph, $k_{\max} = \mathcal{O}(M)$ to the star phase (a small number of stars sharing most of their neighbors) and $k_{\max} = \mathcal{O}(\sqrt{M})$ to the fully connected subgraph. (c) The (cumulative) degree distribution at $T = 0.84$ and $t = 600N$ follows a power law. This shows that the degree distribution decays as a power-law with the exponent $\gamma \approx 3$.

indicating that it is a *continuous phase transition*.

For $\Phi_k > 1/2$ Eq. (25) can be used again as a good approximation for the free energy of the graph, since the compact cluster arising from the dispersed state is rather star like. By plugging $f(\Phi_k M) = -(\Phi_k M) \ln(\Phi_k M)$ into that expression, we get

$$F(\Phi_k, T) \approx M(T-1) \ln(N) \Phi_k \quad (27)$$

to leading order, which is linear in Φ_k . In agreement with our observations above, this formula predicts that for $T < 1$ the star is a stable configuration ($\Phi_k=1$ is a minimum of the free energy), and for $T > 1$ it becomes unstable. The transition at $T = T_c = 1$ is thus step-like with no hysteresis, indicating a continuous phase transition with an infinitely large critical exponent. We assume that the observed deviation of T_c from 1 in the MC simulations is a finite size effect.

V.C) Relation to growth with preferential attachment

A remarkable feature of the MC dynamics is that in case of the energy $f(k_i) = -k_i \ln k_i$, by crossing T_c from above, a scale-free graph (with a degree distribution $\sim k^{-\gamma}$ with $\gamma \simeq 3$) appears at some point of the evolution of the graph from the random configuration towards the star. This supports

the notion that scale-free graphs are temporary (dynamical) configurations, not typical in equilibrium distributions. The MC dynamics is governed by the change of the energy associated with the reallocation of an edge. Estimating the energy change of a vertex by the derivative of the single vertex energy $f(k_i) = -k_i \ln(k_i)$, we get $\Delta E = 1 - \ln(k_i)$. Plugging this into the Boltzmann factor, $\exp[-\Delta E/T]$, at $T = T_c = 1$ we get a quantity proportional to k_i for the acceptance/rejection ratio of a randomly selected move. Since the preferential attachment in the Barabási-Albert model [4] is proportional to k_i , *it is natural that our dynamics also produces scale-free graphs.*

Another interesting aspect of the $f(k_i) = -k_i \ln k_i$ energy is that the configurations in the two compact phases resemble the two major graph topologies obtained in Ref. [18], by optimizing the network for local search with congestion. Our intermediate phase with a few large central hubs sharing neighbors is similar to the optimal topology for a small number of parallel searches, whereas the low-temperature configuration, the fully connected subgraph resembles the homogeneous topology optimal for a large number of parallel searches. However, an important difference between the two problems is that in our case a vertex is allowed to lose all of its connections under the restructuring process. The two “similar-to-optimum” configurations appear as a natural consequence of the underlying dynamics. This observation suggests a potential application of the presented theory: tackling problems related to graph topology optimization by simulated annealing techniques.

V. D) Topology-dependent non-extensiveness of the energy

Both types of the single vertex energy functions discussed in the present section lead to compact configurations at low temperatures, for which the most highly connected vertices possess macroscopic numbers of edges. As a consequence, *the energy of the system scales differently with system size at high and low temperatures*, and diverges differently as $N \rightarrow \infty$. At high temperature, the system consists of many small unlinked clusters of about the same size, therefore a change in the total system size affects only the number of the clusters, and the energy scales as N . On the other hand, when $f(k_i) = -k_i \ln(k_i)$, at low temperatures the energy of the star and the fully connected subgraph scales as $N \ln(N)$; in case of $f(k_i) = -k_i^2$, the energy of the star scales as N^2 . Thus (unlike, *i.e.*, in the mean-field Ising model), there is *no way to choose an appropriate coupling constant that could render the energy extensive in all topological states simultaneously.*

Nevertheless, the dispersed state (having an extensive graph energy) can equally be studied in the grand canonical ensemble.

VI. THE GRAND CANONICAL ENSEMBLE

In the grand canonical ensemble, the degree distribution can be expressed as [11]

$$P_k = C \frac{e^{-\beta f(k) - \mu k}}{k!}. \quad (28)$$

where C is a normalization factor and the chemical potential μ is adjusted to give the correct $\langle k \rangle$. For $f(k) = -k \ln(k)$, using Stirling’s formula, the distribution takes the form

$$P_k = C \frac{e^{-(\mu-1)k}}{\sqrt{2\pi k}} k^{(1/T-1)k}. \quad (29)$$

When $T > 1$, this has a tail, which decays faster than exponential, consequently, each vertex has a small degree. For $T < 1$, on the other hand, the tail becomes divergent, signaling a phase transition at $T = T_c = 1$. Note however that in the $T < 1$ temperature range, due to the non-extensive contribution of the diverging degrees, the ensembles are not equivalent, and the grand canonical description loses its validity.

At the critical temperature, the grand canonical description might still be valid. Choosing a more general single vertex energy, $f(k_i) = -(k_i - \alpha) \ln(k_i)$, and setting $\langle k \rangle$ such that $\mu = 1$, the degree distribution acquires a power law tail ($P_k \sim k^{-(\alpha+1/2)}$) and the network becomes scale-free at this temperature. We have to stress though that the scale-free network at T_c is not general: for $\mu > 1$ the tail decays exponentially, and for $\mu < 1$ the tail diverges.

VII. SUMMARY

We studied the restructuring in networks using a canonical ensemble, where temperature corresponds to the level of noise in real systems and the energy associated with the different configurations accounts for the advantage gained or lost during the rewiring of the edges. We found that for various types of energies, first order and continuous phase transitions may appear when changing temperatures. In case of the $E = -s_{\max}$ energy, if $\langle k \rangle < 1$, a dispersed-loose phase transition occurs at a finite temperature, equivalent to the percolation phase transition of classical random graphs when $\langle k \rangle$ is varied around $\langle k \rangle = 1$. We obtained a simple expression for the $T_c(\langle k \rangle)$ critical line separating the two phases in the $[\langle k \rangle, T]$ plane from a theoretical analysis of the conditional free energy. For other forms of the energy depending on the size of the largest cluster we found first order phase transitions. We also studied the effects of different single vertex energies, namely the $E = -\sum_i k_i^2$ and $E = -\sum_i k_i \ln(k_i)$ cases. The network in the former case exhibits a first order phase transition from a dispersed state to a star-like state, where nearly all edges are linked to a single vertex. With the $-\sum_i k_i \ln(k_i)$ energy, the dispersed state transforms into a compact one with a few large stars via a continuous phase transition. In the critical point, scale-free networks can be recovered. At lower temperatures another transition occurs (this

time of first order), where the configuration is turned into a fully connected subgraph.

Although in this paper we assumed that $\langle k \rangle \leq 1$, this is not a necessary requirement, when the energy is assigned to individual vertices. For large average degree ($\langle k \rangle > 2$) the only difference is that one vertex cannot collect all the edges, and thus, several stars appear in the “star” configuration. Further interesting directions in the context of the above study include the investigation of additional relevant forms for the energy [e.g., $E = (k - n)^2$ with $n > 1.5$] and the joint effects of restructuring and growth.

VIII. ACKNOWLEDGMENTS

The authors are grateful to Gábor Tusnády for many valuable discussions. This research has been supported by the Hungarian Scientific Research Fund under grant No: OTKA 034995. I. F. acknowledges a scholarship from the Communication Networks Laboratory at ELTE.

-
- [1] A.-L. Barabási and R. Albert, *Rev. Mod. Phys.* **74**, 47 (2002).
 - [2] S. N. Dorogovtsev and J. F. F. Mendes, *Evolution of Networks: From Biological Nets to the Internet and WWW* (Oxford University Press, 2003).
 - [3] D. J. Watts and S. H. Strogatz, *Nature* **393**, 440-442 (1998).
 - [4] A.-L. Barabási and R. Albert, *Science* **286**, 509 (1999).
 - [5] P. Erdős and A. Rényi, *Publ. of the Math. Inst. of the Hung. Acad. of Sci.* **5**, 17-61 (1960).
 - [6] B. Bollobás, *Graph Theory, An Introductory Course* (Springer-Verlag, Berlin, 1979).
 - [7] G. Bianconi and A.-L. Barabási *Phys. Rev. Lett.* **86**, 5632 (2001).
 - [8] D. Stark and B. Vedres, Santa Fe Institute working paper, (2003).
 - [9] Z. Burda, J. D. Correia, and A. Krzywicki, *Phys. Rev. E* **64**, 046118 (2001).
 - [10] Z. Burda and A. Krzywicki, *Phys. Rev. E* **67**, 046118 (2003).
 - [11] J. Berg and M. Lässig, *Phys. Rev. Lett.* **89**, 228701 (2002).
 - [12] M. Baiesi and S. S. Manna, *cond-mat/0305054* (2003).
 - [13] A. D. Sánchez, J. M. López, and M. A. Rodríguez, *Phys. Rev. Lett.* **88**, 048701 (2002).
 - [14] K. Klemm, V. M. Eguíluz, R. Toral, and M. S. Miguel, *Phys. Rev. E* **67**, 026120 (2003).
 - [15] A. V. Goltsev, S. N. Dorogovtsev, and J. F. F. Mendes, *Phys. Rev. E* **67**, 026123 (2003).
 - [16] G. Szabó, M. Alava, and J. Kertész, *Phys. Rev. E* **67**, 056102 (2003).
 - [17] G. Mukherjee and S. S. Manna, *Phys. Rev. E* **67**, 012101 (2003).
 - [18] R. Guimerá, A. Díaz-Guilera, F. Vega-Redondo, A. Cabrales and A. Arenas, *Phys. Rev. Lett.* **89**, 248701-1 (2002).
 - [19] S. Valverde, R. Ferrer Cancho and R. V. Solé, *Europhysics Lett.* **60**, 512 (2002).
 - [20] I. Derényi, I. Farkas, G. Palla and T. Vicsek, submitted to *Phys. Rev. Lett.*
 - [21] N. Metropolis, A. W. Rosenbluth, M. N. Rosenbluth, A. H. Teller and E. Teller, *Journal of Chemical Physics* **21**, 1087

(1953).

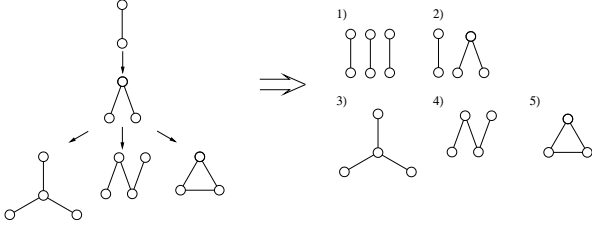
- [22] A. Ramezanpour, V. Karimipour, and A. Mashaghi, *Phys. Rev. E* **67**, 046107 (2003).
- [23] D. Bennett-Wood, I. G. Enting, D. S. Gaunt, A. J. Guttmann, J. L. Leask, A. L. Owczarek, S. G. Whittington, *J. Phys. A* **31**, 4725 (1998).
- [24] D. C. Hong, S. Havlin, H. J. Herrmann, H. E. Stanley, *Phys. Rev. B* **30**, 4083 (1984).
- [25] D. ben-Avraham and S. Havlin, *Diffusion and Reactions in Fractals and Disordered Systems* (Cambridge University Press, 2000).
- [26] P. Devillard and H. E. Stanley, *Phys. Rev. A* **41**, 2942 (1989).
- [27] K. Hukushima, *Comp. Phys. Comm.* **147**, 77 (2002).
- [28] M. E. J. Newman, *SIAM Rev.* **45**, 167 (2003).
- [29] B. Bollobás, *Random Graphs* Cambridge University Press (2001).
- [30] M. E. J. Newman, S. H. Strogatz, and D. J. Watts, *Phys. Rev. E* **64**, 026118 (2001).
- [31] To judge the density of interactions, recall that among the sites of the underlying lattice – *i.e.*, the edges of the complete graph with N vertices – there are only first and second neighbors. One lattice site (one edge of the complete graph) has $2(N - 2)$ first neighbors and $N^2/2 - 5N/2 + 3$ second neighbors.

APPENDIX A

In the exact enumeration method, as mentioned in sec.III.A, the first step is to generate all connected graphs with $m + 1$ edges from the connected graphs with m edges, either by connecting a new vertex to the core or by introducing a new link. In order to avoid double counting, every new graph obtained this way is compared one by one to all already revealed topologies using the following algorithm. Two graphs of identical topology have identical degree distribution also, therefore this property is checked first. In case of perfect match, the vertices in both graphs are labeled in such a way, that a given index belongs to vertices with equal number of links in the two graphs. Next, for each index in one graph, the set of the neighbors indices is compared to its equivalent index set in the other graph. If not all sets are identical, then the labels in one of the graphs have to be permuted until perfect match between the neighboring relations is reached. (Obviously, labels are interchanged between vertices of same degree only). If the perfect match in the neighboring relations cannot be achieved for any permutation of the indices, the two graphs are of different topology.

When a new topology is obtained, the corresponding combinatorial factors can be generated in a similar manner, by counting the number of permutations of the indices in the graph that lead to the same neighboring relations (same neighboring index sets) as the original indexing.

As a simple example, we demonstrate the evaluation of \mathcal{N}_α for all states in case of $M = 3, N \geq 6$. The construction of the connected graphs, and the possible topologies are shown below:



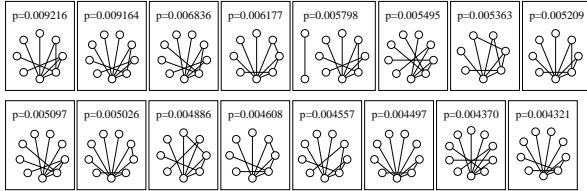
In case of a topology that does not possess any symmetries, \mathcal{N} is simply $N!/(N - N_t)!$, where N_t is the number of vertices included in the topology. In general this initial \mathcal{N} has to be further divided by the number of those permutations of the indices of the vertices that leave the topology unchanged. Therefore, if the topology contains n identical subgraphs (like in case of state $\alpha = 1$ above, where the topology is built up from three identical subgraphs) the initial value of \mathcal{N} has to be divided by $n!$. Furthermore, if any subgraph in the topology remains unchanged for l permutations of the indices within itself, \mathcal{N} has to be divided by l . In the example above, for the states $\alpha = 1$ and $\alpha = 2$, for all subgraphs, $l = 2$, in case of the states $\alpha = 3$ and $\alpha = 5$, $l = 3!$, and for the state $\alpha = 4$, $l = 2$.

Altogether, in the chosen case, the \mathcal{N} of the five possible states can be expressed as

$$\mathcal{N}_1 = \frac{N!}{(N-6)!2^3 3!}, \quad \mathcal{N}_2 = \frac{N!}{(N-5)!2^2},$$

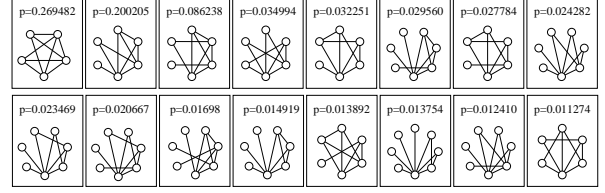
$$\mathcal{N}_3 = \frac{N!}{(N-4)!3!}, \quad \mathcal{N}_4 = \frac{N!}{(N-4)!2}, \quad \mathcal{N}_5 = \frac{N!}{(N-3)!3!}.$$

To provide a simple example of an application, we show the first few most probable states in case of $E = -\sum k_i \ln k_i$ at $T = 0.65$:



When the temperature is lowered to $T = 0.3$, these are

replaced by the following graphs:



APPENDIX B

For simplicity, we shall consider tree like clusters only and neglect the clusters with loops. Since the chances of a component containing a closed loop of edges goes as N^{-1} when $\langle k \rangle < 1$ and no giant connected component can be found in the system, this is a valid approximation in the thermodynamic limit [30]. The number of possible trees of size s in an undirected network can be estimated as follows. We pick a random realization of a tree sized s (meaning s edges and $s + 1$ vertices), and we choose a vertex in it to be the ‘‘root’’ of the tree. Starting from this root, we descend through all possible paths until we reach all the branches, and on the way we replace the undirected edges with directed ones pointing from the vertex closer to the root towards the vertex farther away from the root. This procedure results in a directed tree, where each vertex (except the root) has one and only one incoming edge and $n \geq 0$ outgoing edges. Then, another realization of a tree can be obtained from the present one by choosing a vertex, and moving the other end of the incoming edge from its original place to a new vertex. Of course, this new vertex cannot be one of the ‘‘descendants’’ of the selected vertex, since that way we would create a loop and split the tree into two unconnected parts. Nevertheless, if s is large enough, for the majority of the vertices this restriction eliminates only a negligible part of the possible rewirings. Therefore we may estimate the number of possible new trees obtained from the rewiring of the incoming edge of a single vertex by s , and the total number of trees of size s by s^s .